

Mechanical Environment Modulates Biological Properties of Oligodendrocyte Progenitor Cells

Anna Jagielska,^{1,*} Adele L. Norman,^{2,*} Graeme Whyte,^{3,*†} Krystyn J. Van Vliet,¹
Jochen Guck,^{3,4} and Robin J.M. Franklin²

Myelination and its regenerative counterpart remyelination represent one of the most complex cell–cell interactions in the central nervous system (CNS). The biochemical regulation of axon myelination via the proliferation, migration, and differentiation of oligodendrocyte progenitor cells (OPCs) has been characterized extensively. However, most biochemical analysis has been conducted *in vitro* on OPCs adhered to substrata of stiffness that is orders of magnitude greater than that of the *in vivo* CNS environment. Little is known of how variation in mechanical properties over the physiological range affects OPC biology. Here, we show that OPCs are mechanosensitive. Cell survival, proliferation, migration, and differentiation capacity *in vitro* depend on the mechanical stiffness of polymer hydrogel substrata. Most of these properties are optimal at the intermediate values of CNS tissue stiffness. Moreover, many of these properties measured for cells on gels of optimal stiffness differed significantly from those measured on glass or polystyrene. The dependence of OPC differentiation on the mechanical properties of the extracellular environment provides motivation to revisit results obtained on nonphysiological, rigid surfaces. We also find that OPCs stiffen upon differentiation, but that they do not change their compliance in response to substratum stiffness, which is similar to embryonic stem cells, but different from adult stem cells. These results form the basis for further investigations into the mechanobiology of cell function in the CNS and may specifically shed new light on the failure of remyelination in chronic demyelinating diseases such as multiple sclerosis.

Introduction

MYELINATION, THE PROCESS IN WHICH axons are wrapped with a lipid-rich sheath of multiple membrane layers called myelin, constitutes one of the most important developments in vertebrate evolution and is amongst its most complex cell-to-cell interaction [1]. Myelin allows axons to conduct action potentials by the rapid and efficient process of saltatory conduction and also confers an important supportive effect on the underlying axon, both of which have allowed vertebrates to grow to much larger sizes and to function at a higher cognitive level than would have been possible in its absence.

Myelin in the central nervous system (CNS) is produced by oligodendrocytes (OLs) that are generated during the perinatal period from a population of multipotent progenitor cells called oligodendrocyte progenitor cells (OPCs). During development, OPCs are generated from distinct germinal

zones [2], while in the adult, they constitute an abundant, widely distributed and self-renewing population of cells manifesting features of an adult neural stem cell population [3–6]. It is these adult cells that are responsible for generating new OLs during remyelination [6,7]. Newly generated OLs reinvest demyelinated axons in a spontaneous, but inconsistent regenerative process called remyelination, the therapeutic promotion of which is a key current objective in regenerative medicine [8].

Both the developmental process of myelination and the regenerative process of remyelination involve proliferation and migration of OPCs before they differentiate into OLs that engage axons, wrapping them with a membranous process that ultimately forms the myelin sheath. Understanding the mechanisms of these diverse aspects of myelin sheath formation constitutes a major challenge for developmental neurobiology and is a prerequisite for developing

¹Department of Materials Science and Engineering & Department of Biological Engineering, Massachusetts Institute of Technology, Cambridge, Massachusetts.

²Cambridge Stem Cell Institute & Department of Veterinary Medicine, University of Cambridge, Cambridge, United Kingdom.

³Cavendish Laboratory, Department of Physics, University of Cambridge, Cambridge, United Kingdom.

⁴Biotechnology Center, Technische Universität Dresden, Dresden, Germany.

*These authors contributed equally to this work.

†Present affiliation: Department of Physics, University Erlangen-Nuremberg, Erlangen, Germany.

effective remyelination therapies. Each of these events involves cells mechanically interacting with and physically engaging the local environment. However, while the biochemical-signaling governing myelination has been explored extensively [9], it is not known whether the mechanical properties of both the cells and the environment with which they interact contribute to the orchestration of this process. This question is of fundamental importance, since much of our understanding of OL biology is inferred from cell culture studies using substrata such as glass or polystyrene (PS) that are orders of magnitude stiffer than any material found in the body, particularly those in the CNS (Fig. 1e). In this study, we consider whether OPCs are responsive to mechanical surroundings by studying the effect of *in vitro* substratum (a flexible cell culture surface) stiffness on cell stiffness, adhesion, survival, proliferation, migration, and differentiation, using a combination of atomic force microscopy (AFM), immunocytochemistry,

and time-lapse optical microscopy. Our results show that cells of the OL lineage are mechanoresponsive and that substrata of different compliance are optimal for specific cellular processes. These findings support the hypothesis that mechanical cues are likely to contribute to regulation of myelin sheath formation in the developing and demyelinated CNS and need to be considered for successful remyelination therapies.

Materials and Methods

Cell culture

All chemicals were obtained from Sigma Aldrich unless otherwise stated. OPCs were isolated from Sprague Dawley rodent mixed glial cultures, as previously described [10]. Briefly, mixed glial cultures established from neonatal cortices were maintained in 10% fetal bovine serum for 10–14 days before overnight shaking to remove OPCs. OPCs were

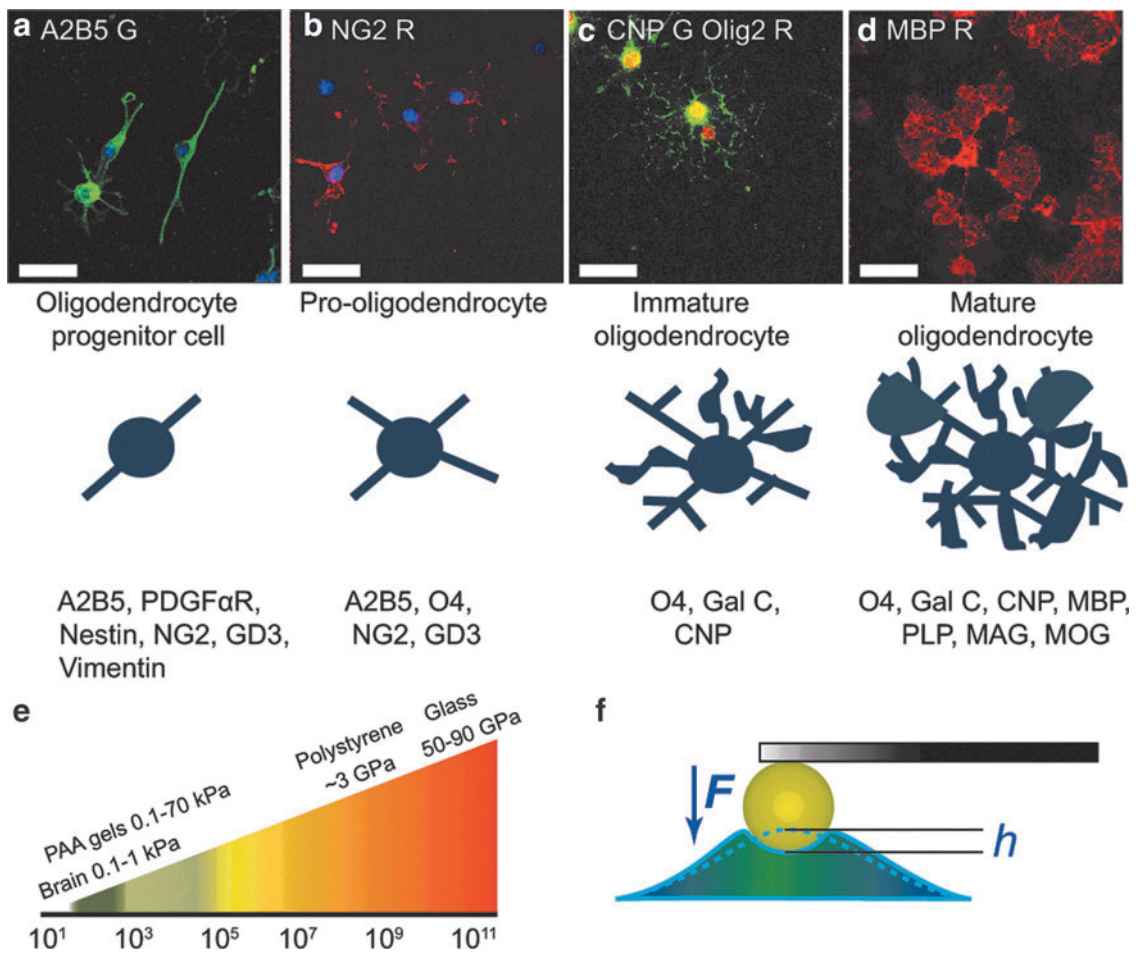


FIG. 1. Oligodendrocyte lineage differentiation markers and tissue stiffness. **(a–d)** oligodendrocyte progenitor cells (OPCs) *in vitro* undergo well characterized morphological changes (schematics) and express multiple differentiation markers. OPCs were isolated at the precursor stage where they expressed A2B5 (green, **a**) and NG2 (red, **b**) and had a simple bi- or multipolar shape. After induction of differentiation, cells reached the pro-oligodendroblast stage expressing 2',3'-cyclic nucleotide 3'-phosphohydrolyase (CNP) (green, **c**) and increasing in morphological complexity. Beyond 5 days postinduction, many cells had lost defined processes and had elaborated a myelin membrane (myelin basic protein [MBP] red, **d**). Scale bars 25 μ m. **(e)** Comparison of stiffness range (Young's modulus, Pa) of brain tissue, polyacrylamide (PAAm) gels used in this work, polystyrene (PS), and glass; **(f)** Schematic representation of atomic force microscopy (AFM)-enabled nanoindentation of a cell via a cantilevered spherical bead; F is applied force and h is indentation depth. Color images available online at www.liebertpub.com/scd

maintained in a progenitor state in the DMEM (Invitrogen) with Sato's modification (5 $\mu\text{g}/\text{mL}$ insulin, 50 $\mu\text{g}/\text{mL}$ holo-transferrin, 5 ng/mL sodium selenate, 16.1 $\mu\text{g}/\text{mL}$ putrescine, 6.2 ng/mL progesterone, and 0.1 mg/mL bovine serum albumin) plus 10 ng/mL platelet-derived growth factor homodimer AA (PDGF-AA) and 10 ng/mL basic fibroblast growth factor-2 (FGF-2; Peprotech) (PDGF-AA and FGF-2 were refreshed daily) (proliferation medium). The growth factors PDGF-AA and FGF-2 are physiological and pathophysiological OPC mitogens and enhancers of migration, which in combination also maintain OPCs in an undifferentiated state. To induce differentiation, OPCs were cultured in Sato's medium without PDGF-AA or FGF-2, plus 30 ng/mL tri-iodothyronine, 63 $\mu\text{g}/\text{mL}$ N-acetyl cysteine, and 0.36 ng/mL hydrocortisone (differentiation medium).

Functionalization of glass and PS dishes

Tissue culture PS (BD Falcon) and glass coverslips were incubated for 1 h at 37°C with 5 $\mu\text{g}/\text{mL}$ (PS) or 50 $\mu\text{g}/\text{mL}$ (glass) poly-D-lysine (PDL, 70 kDa; Sigma), and washed twice with deionized water before cell seeding.

Polyacrylamide gel preparation

Gels were fabricated onto round 22-mm glass coverslips (for cell adhesion, area, and morphology experiments) or P60 glass-bottom dishes (30-mm glass diameter, Invitro Scientific, for AFM and migration experiments), as described previously [11,12]. For details see Supplementary Information S1 (Supplementary Data available online at www.liebertpub.com/scd).

Antibodies

The primary antibodies used for immunocytochemistry were mouse anti-A2B5 (in house hybridoma), mouse anti-O4 (Millipore), rabbit anti-NG2 (Millipore), mouse anti-CNPase (Millipore), rat anti-MBP (Serotec), and rabbit anti-Ki67 (Thermo Scientific). Secondary antibodies used were goat anti-mouse IgM Alexa 488 (Invitrogen), goat anti-rabbit Alexa 488 (Invitrogen), goat anti-rabbit cy3 (Jackson Immunoresearch), and donkey anti-rat cy3 (Jackson Immunoresearch). Propidium iodide (PI; Invitrogen) was used to measure cell survival. Cells were incubated live with 50 $\mu\text{g}/\text{mL}$ PI for 15 min at 37°C.

Immunocytochemistry

Cells were fixed with 4% paraformaldehyde, washed with phosphate-buffered saline (PBS), and blocked with 3% normal goat serum in PBS and 0.1% Triton \times 100. Primary antibodies were diluted in 3% normal goat serum in PBS and 0.1% Triton \times 100 and incubated at room temperature for 1 h. Coverslips were washed 3 \times with PBS, and secondary antibodies diluted 1:500 in 3% normal goat serum in PBS and 0.1% Triton \times 100, and incubated for 1 h. They were then washed and nuclei were stained with Hoechst (2 $\mu\text{g}/\text{mL}$ in PBS for 5 min). Gels were stored in PBS 0.1% sodium azide and plates sealed with parafilm and stored at 4°C to prevent dehydration. Coverslips were mounted using the Fluoromount G (Southern Biotechnology) mounting medium.

Microscopy and image analysis for cell adhesion, survival, proliferation, and differentiation measurements

Confocal z-stacks of OPCs on glass coverslips were taken using a Leica TCS SP5 microscope. Images of cells on gels were obtained using a Zeiss Axio observer A1 epifluorescence microscope. For the adherence assay, 10 fields/gel at 10 \times magnification were quantified. For Ki67 and PI staining, 5 fields/gel at 20 \times magnification were quantified as percentage of Ki67 or PI positive cells with respect to the total number of cells (identified via Hoechst positive nuclear staining). To assess morphology, the cell area or proportion of MBP⁺ cells, images of 10 fields/gel were taken at 20 \times magnification. The area of 100 cells across 2 gels/condition was measured in each experiment. Data shown are mean \pm standard error of the mean (SEM) and show combined data from a minimum of 3 independent experiments. Cells were counted and the cell area calculated using ImageJ software [13]. To measure the area, manual thresholding was performed and individual cells outlined before using the Measure Area function.

AFM-based measurements of cell stiffness

All AFM-enabled indentation measurements of cell elastic modulus and creep compliance were done with an MFP-3D Bio AFM (Asylum Research), using a silicone nitride cantilever with an attached PS bead of 25- μm diameter and a nominal spring constant $k=0.03\text{ N/m}$. The actual spring constant was calibrated via the thermal noise method [14]. Cells were measured at 37°C in the HEPES buffer-based medium at pH 7.4.

Elastic modulus. The Young's elastic modulus of cells was measured for 106 OPCs and 110 OLs adhered to a PDL-coated PS dish. Twenty-five force-indentation curves were collected for each cell at its center, the indentation elastic modulus E was calculated by fitting the Hertz model [15] for an indentation depth of 0.4 μm ; the values for each cell were averaged for the elastic modulus reported. Probe retraction was triggered after reaching the maximum force of 350 pN; the cantilever base velocity was 4 $\mu\text{m}/\text{s}$.

Creep compliance. For each cell, 5 indentation depth versus time responses ($h-t$) were obtained by applying a constant force of 150 pN for 20 s to the center of each cell. Forty OPCs and 40 OLs were measured for each substratum condition. $h-t$ curves measured for individual cells were averaged over the entire data set (Supplementary Fig. S1). The average $h-t$ curve for each cell was transformed to its reciprocal, $J(t)^{-1}$, which is proportional to a time-dependent modulus, $E(t) = 2(1 + \nu)J(t)^{-1}$ (Poisson ratio of cell assumed $\nu=0.5$) (Fig. 2b, c). $J(t)$ was calculated according to the Lee-Radok solution for creep compliance in shear under spherical indentation [16]: $J(t) = \frac{8\sqrt{R}}{3F_0} h(t)^{3/2}$, where R is a spherical probe radius, F_0 is applied force, and $h(t)$ is indentation depth at time t .

Cell migration measurements

Migration parameters were calculated from 4-h cell paths recorded by time-lapse imaging, with 3-min intervals between snapshots. Cells were measured at 5% CO₂ and 37°C, in the proliferation medium containing the growth factors

PDGF-AA and FGF-2 that are well recognised OPC mitogens and enhancers of migration (imaging was started 1 h after adding a daily dose of 10 ng/mL of PDGF-AA and FGF-2 to the media). For each substratum, 30 OPCs per experiment were measured at different locations of a gel surface, experiments were repeated twice, and data were averaged over the entire set of 60 cells. From these paths, accumulated distance (sum of distances traveled at each interval), start-to-end distance (shortest distance between starting and final position), directionality (start-to-end distance/accumulated distance), velocity (calculated as an average over all 3-min interval velocities), and radius of migration (maximum distance traveled from the starting location) were computed using ImageJ software [13] with module “Analyze Particles” to determine coordinates of the cell centroid in each snapshot.

Statistical analysis of data

For the cell adhesion, survival, proliferation, and differentiation experiments, the reported errors were SEM. A statistical significance analysis was done by the Krushal Wallis analysis of variance and Dunn’s *post hoc* tests. For the cell stiffness and migration experiments, reported errors are SEM estimated by bootstrapping, and statistical significance was analyzed by hypothesis-testing with bootstrapping (Supplementary Information S2).

Results

OPCs can be grown and differentiated on substrata of different stiffness

To investigate the effect of mechanical stimulation on cells of the OL lineage, primary rat OPCs were cultured on polyacrylamide (PAAm) gels coated with PDL. The proportions of PAAm and Bis-A cross linker were varied to cover a range of Young’s elastic moduli E from 0.1 to 70 kPa, which includes the stiffness range of the human brain tissue ($E \sim 0.1$ –1 kPa; [17–20]) (Fig. 1e). Gel stiffness was confirmed

via both AFM-enabled nanoindentation and bulk rheological measurements (see Supplementary Information, Supplementary Table S1).

OPCs were cultured in the presence of soluble PDGF-AA and FGF-2 to maintain cells in an undifferentiated state [21–24]. Cells displayed a bipolar or simple multipolar phenotype and expressed the OPC markers A2B5 (Fig. 1a) and NG2 (Fig. 1b). Differentiation was induced by withdrawal of PDGF-AA and FGF-2: after ~ 3 days cells were multipolar and expressed the early myelin protein CNPase (Fig. 1c), while after day 3–5 many cells expressed the myelin basic protein (MBP, the marker of mature OLs), and individual processes were replaced by an extensive myelin membrane (Fig. 1d). Hereafter, we refer to cells in this later stage of biochemically induced differentiation as OLs.

OPCs stiffen during differentiation independently of substratum stiffness

Cell stiffness may correlate with the capacity to migrate through tissue [25], and changes in cell stiffness can also correlate with an altered response of cells to external forces [26], which could ultimately contribute to regulation of cell function and differentiation. In development, OPCs migrate through a dense network of neurons and radial glia, and are thus subjected to a range of mechanical forces. In contrast, OLs do not migrate and instead establish stable adhesion to, and myelination of axons, encountering stresses associated with wrapping multiple layers of membrane around each axon [1,27,28]. To test whether this differential function is reflected in the mechanical properties of these cells, we measured the stiffness of OPCs and OLs adhered to tissue culture PS dishes, expressed as the indentation elastic modulus E measured via AFM-enabled nanoindentation (Fig. 1f). The average stiffness of OLs was significantly greater ($P < 0.05$) than that of OPCs, and OLs also exhibited a broader distribution of E (Fig. 2a). This increased variation in mechanical stiffness of OLs may be attributed to the heterogeneity among cells in different stages of lineage progression. Moreover, the

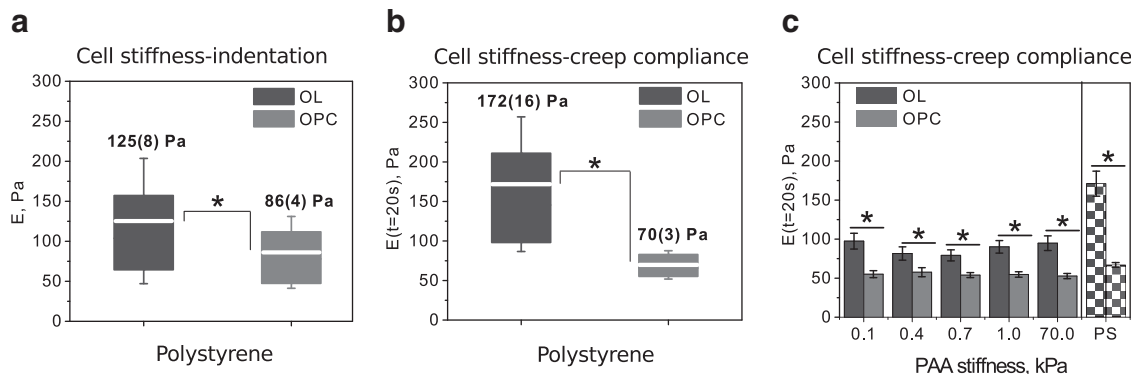


FIG. 2. Stiffness of OPCs and oligodendrocytes (OLs) measured using AFM-enabled nanoindentation. **(a)** Young’s modulus, E , obtained from force–distance indentation curves, for OPCs ($N = 106$ cells) and OLs ($N = 110$ cells) grown on PS; boxes are 25 and 75 percentile values, whiskers are standard deviations, white lines denote mean values, also given in the plot with standard error of the mean (SEM) in parentheses. **(b)** Time-dependent elastic modulus $E(t = 20\text{ s})$ based on creep compliance loading applied for 20 s at constant force of 150 pN, for OPCs ($N = 30$ cells) and OLs ($N = 28$ cells) grown on PS. **(c)** Average values of time-dependent elastic modulus $E(t = 20\text{ s})$ based on creep compliance loading applied for 20 s at constant force of 150 pN, for OPCs and OLs ($N = 40$ per gel) grown on PAAm gels of different stiffness; values for PS shown for comparison (for OPCs $N = 30$ cells, for OLs $N = 28$ cells); error bars are \pm SEM; $*P < 0.05$.

range of OPC and OL stiffness (30–150 Pa and 40–210 Pa for OPCs and OLs, respectively; see Fig. 2a) is within the stiffness range for white matter in brain (100–400 Pa; [20]).

Over longer durations of deformation, cells can exhibit viscoelastic (rate-dependent yet reversible) deformation. To mimic the sustained forces that may occur in vivo on the viscoelastic behavior of OPCs and OLs, we conducted AFM-enabled creep compliance measurements. The stiffness difference between the OPCs and OLs grown on PS persisted under this extended exposure to force (Fig. 2b). Here, average stiffness of cells is represented by the time-dependent elastic modulus, $E(t=20\text{ s})$, which is proportional to the reciprocal of creep compliance, $J(t=20\text{ s})^{-1}$ (see Methods). As with the measurements of stiffness under initial loading (Fig. 2a), the stiffness measured via creep compliance also increased with differentiation progression and exhibited a wider distribution for OLs than for OPCs.

To consider whether similar differences in OPC and OL stiffness occur when the substratum stiffness is reduced to physiological levels (rather than using rigid PS substrata), we repeated creep compliance measurements for cells adhered to PAAm gels of stiffness ranging from 0.1–70 kPa (Fig. 2c). Across this range of gel compliance, the average stiffness of the cell population remained significantly larger for OLs than for OPCs ($P < 0.05$) (Fig. 2c, average $E(t)$ at $t=20\text{ s}$). This difference existed at all time points of force duration and increased with time (Supplementary Fig. S1a–h). Cell stiffness did not depend significantly on gel stiffness ($P > 0.05$) for either OPCs or OLs (Fig. 2c). However, both OPCs and OLs

cultured on the much stiffer PS substratum ($E \sim 3\text{ GPa}$) were stiffer than cells grown on this range of PAAm gels (Fig. 2c).

OPC adhesion is independent of substratum stiffness

Cell attachment is required for multiple events, including cell survival, proliferation, and migration [29]. Further, we and others have shown that variation of stiffness of a synthetic substratum alone can alter the efficiency of cell adhesion [30]. To compare the ability of OPCs to adhere to substrata of varying stiffness, cells were added to the medium above PAAm gels or glass coverslips. Following 1 h of incubation on an orbital shaker at 1 Hz, cells were fixed and nuclei were stained with Hoechst. The maximum adhesion was measured for the gel of $E \sim 1\text{ kPa}$, but the differences in adhesion for gels of differing stiffness did not reach statistical significance; adhesion to glass was lower compared to the gel of 1 kPa stiffness (Fig. 3a). These findings for comparable adhesion on PAAm gels of varying stiffness suggest that changes in OPC adherence in vivo may depend more on the biochemistry of cell surface receptor interactions and the composition of the extracellular environment than on its stiffness.

OPC survival and proliferation are optimal on intermediate substratum stiffness

To assess whether gel stiffness affected OPC survival, cells were plated in the proliferation medium (or in the

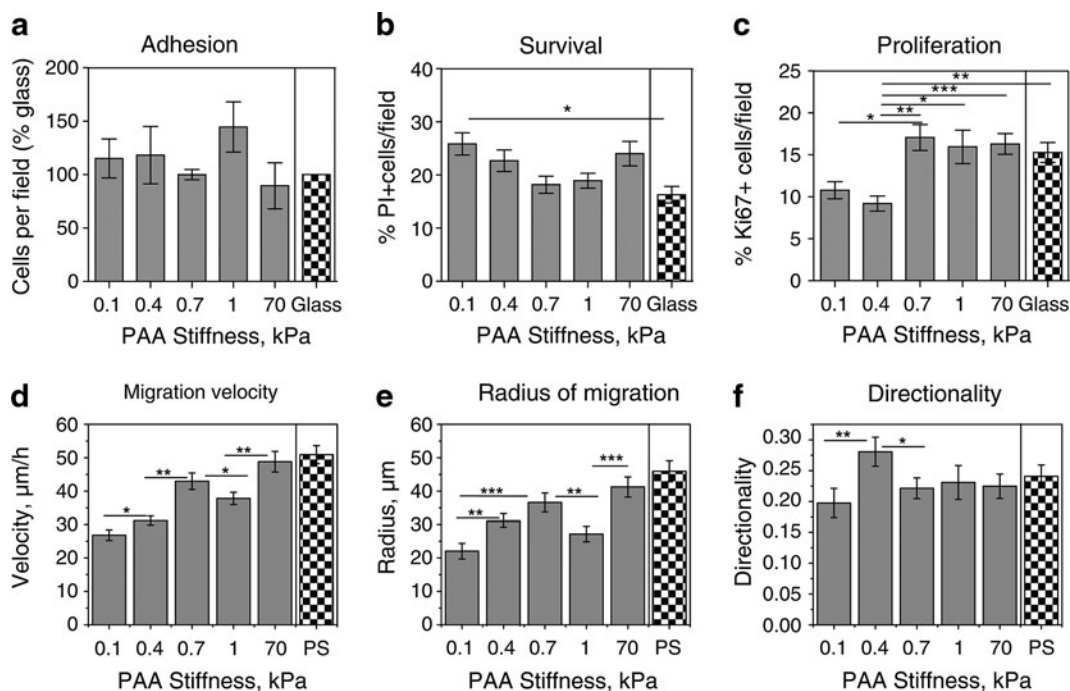


FIG. 3. Influence of stiffness of PAAm gels on adhesion, survival, proliferation, and migration of OPCs. (a) Cell adhesion to PAAm gels quantified after 1 h as percentage of attached cells compared to glass. (b) OPC survival assessed using propidium iodide (PI) labeling of nuclei after 24 h as a proportion of the total number of Hoechst⁺ nuclei. (c) Proliferation assessed as the proportion of Ki67⁺ OPCs compared to total number of nuclei; (d–f) Migration parameters: (d) Velocity; (e) Radius of migration; (f) Directionality; data for PS and glass shown for comparison. For (a–c), data shown are mean from at least 3 experiments (2 gels per condition, 5–10 fields per gel); for (d–f), data are mean for total $N=60$ cells per condition, from 2 experiments. Error bars are \pm SEM; * $P < 0.05$, ** $P < 0.01$, *** $P < 0.001$.

differentiation medium, see Supplementary Information, Supplementary Fig. S2a); pyknotic nuclei of dead or dying cells were labeled with PI after 24h. The percentage of PI-labeled cells with respect to the total number of Hoechst-labeled nuclei was higher on the more compliant gels (0.1 and 0.4 kPa) (Fig. 3b). Within the physiological range of brain tissue stiffness (0.1 to 1 kPa [17–20]), survival was optimal for OPCs on gels of $E \sim 0.7$ and 1 kPa (Fig. 3b).

The percentage of proliferating cells in both the proliferation medium (containing the OPC mitogens PDGF-AA and FGF-2) and the differentiation medium (without PDGF-AA and FGF-2) was measured following immunocytochemistry to the proliferation marker Ki67, 24 h after plating on PAAm gels or glass coverslips. Among the PAAm gels of physiological stiffness, OPCs cultured in the proliferation medium showed an increased proliferation rate on gels of $E \sim 0.7$ and 1 kPa (Fig. 3c), which was significantly greater than on gels of 0.4 and 0.1 kPa. Levels of proliferation were much lower for cells in the differentiation medium, but also for this medium condition the proliferation was highest on gels of $E \sim 0.7$ and 1 kPa (Supplementary Information, Supplementary Fig. S2b). Thus, as with survival, OPC proliferation was greatest on gels within the intermediate range of brain stiffness.

Both OPC proliferation and survival rates measured on glass were similar to those measured on gels of optimal stiffness for these processes ($E \sim 0.7$ –1 kPa) (Fig. 3b, c). However, compared to the glass substrata, there was significantly a lower survival on gels of $E \sim 0.1$ kPa and a decreased proliferation on gels of $E < 0.4$ kPa (Fig. 3b, c).

OPC migration depends on substratum stiffness

Both myelination and remyelination require OPC migration, which could be influenced by the mechanical stiffness of the developing or injured CNS. Analyzing 2-dimensional

migration of these cells along substrata, in the presence of physiological enhancers of OPC migration PDGF-AA and FGF-2, we found that the OPC migration velocity and the radius of migration were maximized on gels of $E \sim 0.7$ kPa (Fig. 3d, e) and the directionality was greatest for gels of $E \sim 0.4$ kPa (Fig. 3f). Other migration parameters, such as accumulated distance and start-to-end distance, were also maximized for gel stiffness of 0.7 kPa (Supplementary Information, Supplementary Fig. S3a, b). For gel substrata with stiffness beyond the physiological range (70 kPa), migration parameters slightly exceeded those for gels of 0.7 kPa stiffness (not statistically significant, $P > 0.05$) (Fig. 3d, e), with exception of directionality, which was independent of substratum stiffness for $E > 0.7$ kPa (Fig. 3f). Thus, within the physiological range of mechanical compliance in the brain, OPC migration was most efficient on gels of intermediate stiffness. As expected, OLs did not migrate on any substrata.

OPCs migrating along PS exhibited larger velocity and radius of migration, but lower directionality as compared to the respective optimal gels ($E \sim 0.7$ kPa for velocity and radius, and 0.4 kPa for directionality) (Fig. 3d–f).

OPC differentiation is enhanced on stiffer substrates

Finally, we tested the influence of substratum stiffness on OPC differentiation by assessing morphology, spread area, and percentage of cells expressing MBP, the mature OL marker. Cells were cultured on PAAm gels of varying stiffness or glass in the differentiation induction medium, and analyzed after 3 days. To assess morphology, cells were costained with antibodies to the OPC marker A2B5 and late progenitor marker O4, and grouped according to phenotypic features: class 1 comprised simple bi- or multi-polar cells that did not have interdigitating processes (Fig. 4a), class 2

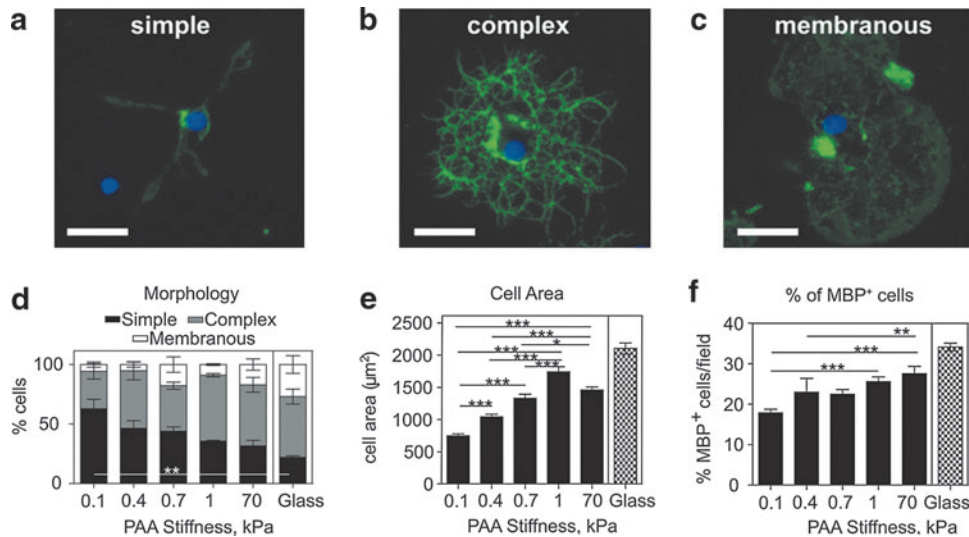


FIG. 4. Influence of gel stiffness on OPC differentiation. (a–c) OPCs and OLs were labeled against A2B5 and O4 and the morphology was assessed using fluorescence microscopy. Morphology was categorized as (a) simple, (b) complex, and (c) membranous; scale bars 25 μm. (d) The percentage of cells in the 3 categories grown on PAAm gels and on glass. (e) Cell area quantified from the fluorescence images and (f) percentage of MBP-expressing cells as a function of substratum stiffness. Data shown are mean of at least 3 experiments (2 gels per condition, 10 fields per gel). Error bars are \pm SEM; * $P < 0.05$, ** $P < 0.01$, *** $P < 0.001$. Color images available online at www.liebertpub.com/scd

comprised complex cells with interdigitating processes, but without membrane sheets (Fig. 4b), and class 3 comprised cells that elaborated a myelin membrane (Fig. 4c). Following 3 days of differentiation, we observed a clear trend in the decreasing fraction of simple cells (class 1, black) and an accompanying increase in the percentage of myelin-producing cells (class 3, white) with increasing substratum stiffness (Fig. 4d). This variation in morphology correlated well with our results for cell spread area, which increased with increasing gel stiffness up to 1 kPa (Fig. 4e). Cell morphology and the surface area were also analyzed at an early stage of differentiation, 1 day postinduction (see Supplementary Information, Supplementary Fig. S2c, d).

As an alternative measure of differentiation, the percentage of MBP-expressing cells was quantified after 3 days postinduction. We again observed a similar trend as for cell morphology and area, with the fraction of MBP-positive cells increasing with increasing gel stiffness (Fig. 4f).

Differentiation within cell cultures on glass at 3 days was higher compared to the optimal gel ($E \sim 1$ kPa), as quantified by morphology, cell area, and %MBP-positive cell assays (Fig. 4d–f).

Discussion

The developmental process of myelination and its regenerative counterpart remyelination require both a sufficient number of OPCs appropriately distributed within the CNS and the differentiation of these progenitor cells into myelin-forming OLs. The mechanisms involved in the regulation of the various cellular events of developmental myelination are among the most extensively explored in neurobiology, and our understanding of the regenerative process has substantially increased in recent years [6,8,31–33]. However, remarkably little is known of how the physical properties of the environment in which these events take place contribute to their regulation, despite the increasing knowledge that tissue cells from other lineages are mechanosensitive [30,34–40] and that physical properties of tissue are profoundly altered by injury [18,41–43] and are therefore likely to have a significant bearing on the efficiency of regeneration. The need for consideration of physical cues becomes acute when one considers that much of what we know about the biology of myelination has been gleaned from tissue culture studies using *in vitro* substrata that are orders of magnitude stiffer than the CNS tissue *in vivo* (Fig. 1e).

Here, we have begun to address this deficit in our understanding of myelination by systematically investigating whether substratum stiffness within the physiological range encountered in the CNS influences OPC survival, proliferation, stiffness, motility, and differentiation. We found that OPC survival, proliferation, and migration (in terms of velocity and distance) occurred at optimal efficiency within the intermediate range of physiological brain tissue stiffness, and that OPC differentiation efficiency increased with increasing substrate stiffness. These data demonstrate that OL lineage cells are mechanosensitive and are therefore likely to be responsive to extracellular mechanical cues. One implication of such mechanosensitivity *in vivo* is that the age-dependent changes of CNS mechanical properties [44] may initially provide ideal conditions for myelination that turn more prohibitive in an adult. Another implication is that patho-

logical changes of the OPCs environment, such as those encountered in demyelinated lesions in multiple sclerosis, may provide a suboptimal mechanical environment that inhibits some OPC functions and contributes directly to inefficient OPC differentiation and remyelination.

Correlations between stem cell stiffness and substratum gel stiffness

We have demonstrated that OPCs are more compliant than OLs, indicating that cell stiffness can vary with differentiation state (Fig. 2a, b). This increased compliance of OPCs might be a physical prerequisite for their efficient migration in a dense 3D environment. OLs on the other hand are nonmigratory, and may therefore not require the same level of compliance [45,46]. However, we found that cell stiffness was independent of gel stiffness: over the range explored, OPC and OL stiffness was statistically invariant with gel stiffness (Fig. 2c). This is in contrast to previous reports for adult mesenchymal stromal cells (MSCs) and fibroblasts, which exhibited increasing cell stiffness with increasing stiffness of similar PAAm gels [38,47]. However, the observed absence of correlation between OPC/OL and gel stiffness is similar to that reported for mouse embryonic stem cells (mESCs) [48]. One plausible reason for this contrasting

TABLE 1. RELATIVE DIFFERENCES BETWEEN CELL PROPERTIES MEASURED ON OPTIMAL GEL AND ON GLASS OR POLYSTYRENE

Cell property	Cell type ^a	Optimal gel stiffness ^b	% Change on optimal gel with respect to glass or polystyrene ^c
Stiffness	OL	e	–48 ^f
	OPC	e	–29 ^f
Adhesion	OPC	1.0 kPa	+45 ^g
Survival	OPC	0.7 kPa	+13 ^g
Proliferation	OPC	0.7 kPa	+13 ^g
Migration—velocity	OPC	0.7 kPa	–17 ^f
Migration—radius	OPC	0.7 kPa	–25 ^f
Migration—directionality	OPC	0.4 kPa	+20 ^f
Differentiation—morphology ^d	OPC/OL	1 kPa	–17 ^g
Differentiation—cell area	OPC/OL	1 kPa	–15 ^g
Differentiation—%MBP expressing cells	OPC/OL	1 kPa	–23 ^g

^aProperties were measured for OPCs, OLs, or in mixed OPC and OL cell culture (OPC/OL).

^bStiffness of PAAm gel on which the property value was maximal.

^cThe % change was calculated as: (value measured on optimal gel – value measured on glass or polystyrene)/(value measured on glass or polystyrene) × 100.

^dCompared is combined percentage of cells with complex and membranous morphology (see Fig. 4) on optimal gel and glass.

^eCell stiffness was independent of gel stiffness, and the average cell stiffness values for gel stiffness range 0.1–1 kPa were used for comparison with polystyrene.

^fMeasurements for cells on polystyrene.

^gMeasurements for cells on glass.

OLs, oligodendrocytes; OPCs, oligodendrocyte precursor cells; MBP, myelin basic protein; PAAm, polyacrylamide gels.

dependence of cell stiffness on gel stiffness is that mESCs and OL lineage cells exhibit a highly rounded cell body with a rather sparse, weakly aligned actin cytoskeleton, in contrast to the well spread, flatter morphology and well-developed actin stress fibers exhibited by MSCs and fibroblasts adhered to increasingly stiff substrata.

Extracellular mechanical environment modulates OPC migration

We found that OPC migration was maximal for gel stiffness of 0.7 kPa, occurring less efficiently on more compliant or stiffer substrata (Fig. 3d, e). During development, OPCs originate within discrete regions from which they migrate throughout the CNS; one may conjecture that this migration is optimized in vivo over only a small range of tissue stiffness that varies both spatially and temporally during development. For example, the stiffness of presumptive white matter tracts, containing radially or longitudinally oriented axons, may provide a more permissive physical environment for OPC migration than the dense network of processes within the gray matter. In support of this, adult white matter is less stiff than adult gray matter [20], although we note that the white matter is already myelinated in the adult brain. The possibility of spatially varied mechanical properties serving as guidance cues for cell migration and behavior in the CNS is a general, emergent theme that is further supported by our results [49]. The underlying molecular mechanisms of how mechanical differences are converted into biochemical signals and ultimately functional changes are currently attracting intense scientific interest [50]. While the elucidation of such mechanisms is beyond the scope of this particular study, these will likely involve ligand–receptor interactions and the actomyosin contractile machinery as discussed for other tissue cell types [51]. Our results demonstrate that such related reports of mechanotransduction are also relevant to cells in the CNS.

Differences between OPC properties measured on substrata of physiological stiffness and on glass or PS

One implication of OPC mechanosensitivity is that some properties measured for cells cultured on PS or glass surfaces, which are orders of magnitude stiffer than brain tissue (~3 and 70 GPa, respectively, compared to <1 kPa; see Fig. 1e), may differ from those occurring in vivo. In Table 1, we summarize relative differences between our results obtained on gels of stiffness optimal for each cell property (i.e., maximizing the magnitude of that property) and on glass or PS. We observed the largest differences for cell stiffness of both OPCs and OLs, which was much lower on gels than on PS. We also observed significantly lower migration velocity and radius on gels compared to that observed on PS, and lower differentiation extent on gels compared to that observed on glass. Cell adhesion was greater on gels than on glass, but cell proliferation and survival did not differ significantly between the optimal gels and glass. It is important to note that PS and glass substrata differ from each other and also from in vivo matrices and in vitro gels in several other characteristics beyond mechanical stiffness (e.g., chemical composition, topography, surface charge, etc.). Thus, our

study here has emphasized correlations between mechanical stiffness and cell responses among substrata of a given class (i.e., PAAm gels of varying stiffness), while noting the additional differences from cell responses observed on conventional glass and PS surfaces.

In conclusion, we have demonstrated that OPCs from the CNS are mechanosensitive. Cell survival, proliferation, migration, and differentiation of these stem cells in vitro all vary significantly with the mechanical stiffness of the environment to which these cells adhere. Note that the survival, proliferation, and migration are maximized at an intermediate gel stiffness over the physiological range considered. In vivo, the mechanical environment of OPCs and OLs is likely to change spatially and temporally, which could plausibly impact differentiation and myelination. Having established the baseline mechanosensitivity of OPCs in quasi-2-dimensional in vitro culture, we and others can now investigate whether local, pathological changes in mechanical environment of the CNS—such as those expected to occur in multiple sclerosis and other demyelinating diseases—may promote dysregulation of OPC differentiation and ultimately lead to incomplete remyelination of lesions. More generally, the mechanical cues accessible to OPCs should be considered together with biochemical cues in further studies of OL function in both healthy brain and demyelinating diseases.

Acknowledgments

We gratefully acknowledge funding from the Human Frontier Science Program, RGP0015. We thank P. Moshayedi, K. Franze and K. Holtzmann for assistance with PAAm gel preparation and rheology experiments, M. Glassman for assistance with rheology experiments, K. Chalut, R. Mahmoodian, and L. Wroblewska for helpful discussions. K.J.V.V. and A.J. thank H. Sullivan for neonatal rat cortex tissue as the source of OPCs.

Author Disclosure Statement

No competing financial interests exist.

References

1. Sherman DL and PJ Brophy. (2005). Mechanisms of axon ensheathment and myelin growth. *Nat Rev Neurosci* 6:683–690.
2. Fancy SP, JR Chan, SE Baranzini, RJM Franklin and DH Rowitch. (2011). Myelin regeneration: a recapitulation of development? *Annu Rev Neurosci* 34:21–43.
3. Kondo T and M Raff. (2000). Oligodendrocyte precursor cells reprogrammed to become multipotential CNS stem cells. *Science* 289:1754–1757.
4. Nunes MC, NS Roy, HM Keyoung, RR Goodman, G McKhann 2nd, L Jiang, J Kang, M Nedergaard and SA Goldman. (2003). Identification and isolation of multipotential neural progenitor cells from the subcortical white matter of the adult human brain. *Nat Med* 9:439–447.
5. Richardson WD, KM Young, RB Tripathi and I McKenzie. (2011). NG2-glia as multipotent neural stem cells: fact or fantasy? *Neuron* 70:661–673.
6. Zawadzka M, LE Rivers, SPJ Fancy, C Zhao, R Tripathi, F Jamen, K Young, A Goncharevich, H Pohl, et al. (2010). CNS-resident glial progenitor/stem cells produce schwann

- cells as well as oligodendrocytes during repair of CNS demyelination. *Cell Stem Cell* 6:578–590.
7. Tripathi RB, LE Rivers, KM Young, F Jamen and WD Richardson. (2010). NG2 glia generate new oligodendrocytes but few astrocytes in a murine experimental autoimmune encephalomyelitis model of demyelinating disease. *J Neurosci* 30:16383–16390.
 8. Franklin RJM and C Ffrench-Constant. (2008). Remyelination in the CNS: from biology to therapy. *Nat Rev Neurosci* 9:839–855.
 9. Miller RH. (2002). Regulation of oligodendrocyte development in the vertebrate CNS. *Prog Neurobiol* 67:451–467.
 10. McCarthy KD and J Devellis. (1980). Preparation of separate astroglial and oligodendroglial cell cultures from rat cerebral tissue. *J Cell Biol* 85:890–902.
 11. Moshayedi P, LD Costa, A Christ, SP Lacour, J Fawcett, J Guck and K Franze. (2010). Mechanosensitivity of astrocytes on optimized polyacrylamide gels analyzed by quantitative morphometry. *J Phys Condens Matter* 22.
 12. Pelham RJ and YL Wang. (1997). Cell locomotion and focal adhesions are regulated by substrate flexibility. *Proc Natl Acad Sci U S A* 94:13661–13665.
 13. Rasband WS. Image J, U. S. National Institutes of Health, Bethesda, Maryland, USA, <http://rsb.info.nih.gov/ij/>, 1997–2008.
 14. Hutter JL and J Bechhoefer. (1993). Calibration of atomic force microscope tips. *Rev Sci Instrum* 64:1868–1873.
 15. Hertz H. (1882). On the contact of rigid elastic solids. *J Reine Angew Math* 92:155–171.
 16. Lee EH and JRM Radok. (1960). The contact problem for viscoelastic bodies. *J Appl Mech* 27:438–444.
 17. Levental I, PC Georges and PA Janmey. (2007). Soft biological materials and their impact on cell function. *Soft Matter* 3:299–306.
 18. Lu YB, K Franze, G Seifert, C Steinhauser, F Kirchhoff, H Wolburg, J Guck, P Janmey, EQ Wei, J Kas and A Reichenbach. (2006). Viscoelastic properties of individual glial cells and neurons in the CNS. *Proc Natl Acad Sci U S A* 103:17759–17764.
 19. Miller K, K Chinzei, G Orsengo and P Bednarz. (2000). Mechanical properties of brain tissue *in-vivo*: experiment and computer simulation. *J Biomech* 33:1369–1376.
 20. Christ AF, K Franze, H Gautier, P Moshayedi, J Fawcett, RJM Franklin, RT Karadottir and J Guck. (2010). Mechanical difference between white and gray matter in the rat cerebellum measured by scanning force microscopy. *J Biomech* 43:2986–2992.
 21. Eccleston PA and DH Silberberg. (1985). Fibroblast growth factor is a mitogen for oligodendrocytes *in vitro*. *Dev Brain Res* 21:315–318.
 22. Milner R, HJ Anderson, RF Rippon, JS McKay, RJM Franklin, MA Marchionni, R Reynolds and C FfrenchConstant. (1997). Contrasting effects of mitogenic growth factors on oligodendrocyte precursor cell migration. *Glia* 19:85–90.
 23. Noble M, K Murray, P Stroobant, MD Waterfield and P Riddle. (1988). Platelet-derived growth factor promotes division and motility and inhibits premature differentiation of the oligodendrocyte type-2 astrocyte progenitor cell. *Nature* 333:560–562.
 24. Bogler O, D Wren, SC Barnett, H Land and M Noble. (1990). Cooperation between two growth factors promotes extended self-renewal and inhibits differentiation of oligodendrocyte-type-2 astrocyte (O-2A) progenitor cells. *Proc Natl Acad Sci U S A* 87:6368–6372.
 25. da Silva J, F Lautenschlager, E Sivaniah and JR Guck. (2010). The cavity-to-cavity migration of leukaemic cells through 3D honey-combed hydrogels with adjustable internal dimension and stiffness. *Biomaterials* 31:2201–2208.
 26. Chowdhury F, YZ Li, YC Poh, T Yokohama-Tamaki, N Wang and TS Tanaka. (2010). Soft substrates promote homogeneous self-renewal of embryonic stem cells via down-regulating cell-matrix tractions. *Plos One* 5:e15655.
 27. Baumann N and D Pham-Dinh. (2001). Biology of oligodendrocyte and myelin in the mammalian central nervous system. *Physiol Rev* 81:871–927.
 28. Bauer NG, C Richter-Landsberg and C Ffrench-Constant. (2009). Role of the oligodendroglial cytoskeleton in differentiation and myelination. *Glia* 57:1691–1705.
 29. Janmey PA, JP Winer, ME Murray and Q Wen. (2009). The hard life of soft cells. *Cell Motil Cytoskeleton* 66:597–605.
 30. Thompson MT, MC Berg, IS Tobias, MF Rubner and KJ Van Vliet. (2005). Tuning compliance of nanoscale polyelectrolyte multilayers to modulate cell adhesion. *Biomaterials* 26:6836–6845.
 31. Franklin RJM and MR Kotter. (2008). The biology of CNS remyelination: the key to therapeutic advances. *J Neurol* 255 (Suppl. 1):19–25.
 32. Patani R, M Balaratnam, A Vora and R Reynolds. (2007). Remyelination can be extensive in multiple sclerosis despite a long disease course. *Neuropathol Appl Neurobiol* 33:277–287.
 33. Patrikios P, C Stadelmann, A Kutzelnigg, H Rauschka, M Schmidbauer, H Laursen, PS Sorensen, W Bruck, C Lucchinetti and H Lassmann. (2006). Remyelination is extensive in a subset of multiple sclerosis patients. *Brain* 129:3165–3172.
 34. Discher DE, P Janmey and YL Wang. (2005). Tissue cells feel and respond to the stiffness of their substrate. *Science* 310:1139–1143.
 35. Engler A, L Bacakova, C Newman, A Hategan, M Griffin and D Discher. (2004). Substrate compliance versus ligand density in cell on gel responses. *Biophys J* 86:617–628.
 36. Engler AJ, MA Griffin, S Sen, CG Bonnemann, HL Sweeney and DE Discher. (2004). Myotubes differentiate optimally on substrates with tissue-like stiffness: pathological implications for soft or stiff microenvironments. *J Cell Biol* 166:877–887.
 37. Engler AJ, F Rehfeldt, S Sen and DE Discher. (2007). Microtissue elasticity: measurements by atomic force microscopy and its influence on cell differentiation. *Methods Cell Biol* 83:521–545.
 38. Engler AJ, S Sen, HL Sweeney and DE Discher. (2006). Matrix elasticity directs stem cell lineage specification. *Cell* 126:677–689.
 39. Flanagan LA, YE Ju, B Marg, M Osterfield and PA Janmey. (2002). Neurite branching on deformable substrates. *Neuroreport* 13:2411–2415.
 40. Richert L, AJ Engler, DE Discher and C Picart. (2004). Elasticity of native and time-linked polyelectrolyte multilayer films. *Biomacromolecules* 5:1908–1916.
 41. Fawcett JW and RA Asher. (1999). The glial scar and central nervous system repair. *Brain Res Bull* 49:377–391.
 42. Lu YB, I Iandiev, M Hollborn, N Korber, E Ulbricht, PG Hirrlinger, T Pannicke, EQ Wei, A Bringmann, et al. (2010). Reactive glial cells: increased stiffness correlates with increased intermediate filament expression. *FASEB J* 25:624–631.
 43. Lucchinetti C, W Bruck, J Parisi, B Scheithauer, M Rodriguez and H Lassmann. (1999). A quantitative analysis of oligodendrocytes in multiple sclerosis lesions. A study of 113 cases. *Brain* 122 (Pt 12):2279–2295.

44. Elkin BS, A Ilankovan and B Morrison 3rd. (2010). Age-dependent regional mechanical properties of the rat hippocampus and cortex. *J Biomech Eng* 132:011010.
45. Lautenschlager F, S Paschke, S Schinkinger, A Bruel, M Beil and J Guck. (2009). The regulatory role of cell mechanics for migration of differentiating myeloid cells. *Proc Natl Acad Sci U S A* 106:15696–15701.
46. Guck J, F Lautenschlager, S Paschke and M Beil. (2010). Critical review: cellular mechanobiology and amoeboid migration. *Integr Biol (Camb)* 2:575–583.
47. Solon J, I Levental, K Sengupta, PC Georges and PA Janmey. (2007). Fibroblast adaptation and stiffness matching to soft elastic substrates. *Biophys J* 93:4453–4461.
48. Poh YC, F Chowdhury, TS Tanaka and N Wang. (2010). Embryonic stem cells do not stiffen on rigid substrates. *Biophys J* 99:L19–L21.
49. Franze K and J Guck. (2010). The biophysics of neuronal growth. *Rep Prog Phys* 73:094601.
50. Dupont S, L Morsut, M Aragona, E Enzo, S Giullitti, M Cordenonsi, F Zanconato, J Le Digabel, M Forcato, et al. (2011). Role of YAP/TAZ in mechanotransduction. *Nature* 474:179–183.
51. Wozniak MA and CS Chen. (2009). Mechanotransduction in development: a growing role for contractility. *Nat Rev Mol Cell Biol* 10:34–43.

Address correspondence to:
Prof. Jochen Guck
Biotechnology Center
Technische Universität Dresden
Tatzberg 47/49
01307 Dresden
Germany

E-mail: jochen.guck@biotec.tu-dresden.de

Received for publication April 09, 2012

Accepted after revision May 30, 2012

Prepublished on Liebert Instant Online XXXX XX, XXXX